2011 IEEE/RSJ International Conference on
Intelligent Robots and Systems
September 25-30, 2011. San Francisco, CA, USA

Bipedal walking control based on Capture Point dynamics

Johannes Englsberger, Christian Ott, Maximo A. Roa, Alin Albu-Schäffer, and Gerhard Hirzinger

***Abstract*— This paper builds up on the Capture Point concept and exploits the simple form of the dynamical equations of the Linear Inverted Pendulum model when formulated in terms of the center of mass and the Capture Point. The presented methods include (i) the derivation of a Capture Point (CP) control principle based on the natural dynamics of the linear inverted pendulum (LIP), which stabilizes the walking robot and motivates (ii) the design of a CP tracking and a CP end-of-step controller. The exponential stability of the CP control law is proven. Tilting is avoided by proper projection of the commanded zero moment point. The robustness of the derived control algorithms is analyzed analytically and verified in simulation and experiments.**

I. Introduction

Scientific visions, such as planetary exploration and service robots, generate the demand of locomotion machines, capable of moving through rough terrain and the natural environment of humans. In this context, the ability to step over small obstacles and the small support area motivate the use of multi-legged and bipedal robots instead of wheel based mobile robots.

From a modeling and control point of view, legged robots offer additional challenges like varying constraints on the ground reaction force as well as under-actuation in the control input depending on the contact situation. As a consequence, the use of simplified models for the control, which incorporate only some essential aspects of the complicated multi-body dynamics, can be useful. The problem of balancing over a limited support area can be well understood using conceptually simple models based on the center of mass (COM) dynamics and its relation to the ground reaction force. Vukobratovic [1] introduced the Zero Moment Point (ZMP) as a concise representation of the vertical force distribution between the foot and the ground. Despite their known limitations, simplified models which relate the COM motion to the ZMP proved to be useful for trajectory generation and gait stabilization in several biped robots [2], [3], [4], [5], [6].

Kajita et al. [2] proposed an extension of the LQR controller by future reference values for the generation of walking patterns. This approach was extended into a linear model predictive controller by Wieber [6] allowing for explicit integration of constraints on the ZMP as well as footstep adaptation.

Choi et al. [5] presented a stability analysis for a ZMP based balancing controller. In [7], a first order model of the ZMP lag is considered in the design of a linear inverted pendulum tracking controller. Sugihara [4] considers the finite support area in the parametrization of the stabilizing controller.

All authors are with Institute of Robotics and Mechatronics, German Aerospace Center, 82234 Weßling, Germany. E-mail: johannes.englsberger@dlr.de

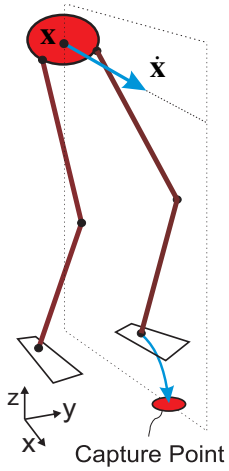

Fig. 1. Illustration of Capture Point

Fig. 2. DLR Biped

Pratt et al. [8] and Hof [9] independently introduced the (LIP based) Capture Point (CP), called 'extrapolated center of mass' in [9]. Intuitively speaking, the CP is the point on the floor onto which the robot has to step to come to a complete rest (Fig. 1). While Pratt et al. discussed its significance for bipedal push recovery, Hof used this concept for designing step-to-step walking controllers. The key issue of the present paper is the rigorous use of the CP and its underlying dynamic structure for bipedal walking control. Our experimental platform is the DLR Biped [10] (Fig. 2), a walking robot which can be both position and torque controlled. For the current work the DLR Biped is operated position-controlled in order to allow a comparison of the CP approach with state of the art ZMP control. We introduce a walking controller based on the CP and the natural dynamics of the LIP.

This paper is organized as follows: Section II derives the Linear Inverted Pendulum (LIP) model, the Capture Point (CP) and its dynamics. Section III introduces a control law based on the CP and the natural LIP dynamics, proves its exponential stability and illustrates related issues of the CP control and tilting avoidance. Section V shows simulation and experimental results, demonstrating the robustness of the CP control and comparing it to preview control [2]. Section VI discusses the potential of CP control. Section VII concludes the paper.

978-1-61284-456-5/11/$26.00 ©2011 IEEE

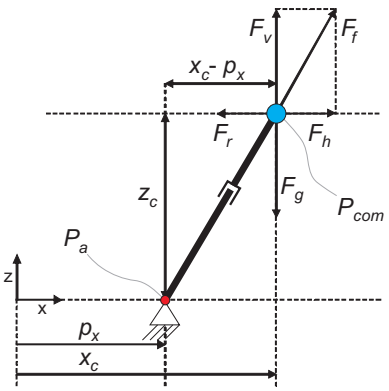

Fig. 3. Linear Inverted Pendulum model

II. Modeling

A. Linear Inverted Pendulum (LIP) Model

The linear inverted pendulum (LIP) model is widely used for the control of bipedal walking robots [3], [4], [5], [11]. It uses the following assumptions:

- the robot is modeled as a point mass corresponding to the center of mass (COM)
- the center of mass is held at constant height z_c
- the base joint of the pendulum is torque free

With these assumptions, the dynamic equations of the robot are linear and decoupled, which makes the use of the LIP model so attractive. Decoupling means that all equations derived below for one dimension can be used equivalently and independently for both horizontal components (x and y, Fig. 1) of the system dynamics. Fig. 3 gives an overview of the LIP model. The COM position is given by $P_{com} = [x_c, z_c]^T$. $P_a = [p_x, 0]^T$ is the position of the torque-free pendulum base joint, which is equivalent to the Zero Moment Point (ZMP [1]) in a robot. The ground reaction force F_f acting on the COM is collinear with the vector $(P_{com} - P_a)$ because the base joint of the pendulum is torque-free. F_v is the vertical component of F_f. It compensates for the gravitational force F_g acting on the COM. The inertial force $F_r = m\,\ddot{x}_c$ completes the equilibrium of forces in P_{com}. By comparison of the force parallelogram and the geometrical parallelogram we find

$$\frac{F_h}{F_v} = \frac{F_r}{F_g} = \frac{m\,\ddot{x}_c}{m\,g} = \frac{x_c - p_x}{z_c} \tag{1}$$

Therefore, an expression for the horizontal acceleration of the COM is

$$\ddot{x}_c = \omega^2\,(x_c - p_x) \tag{2}$$

where $\omega = \sqrt{g/z_c}$ and p_x is the x-coordinate of the ZMP. ω is assumed to be positive throughout the paper. The complete system dynamics of the LIP model is given by

$$\dot{\sigma} = \begin{bmatrix} 0 & 1 \\ \omega^2 & 0 \end{bmatrix} \sigma + \begin{bmatrix} 0 \\ -\omega^2 \end{bmatrix} p_x \tag{3}$$

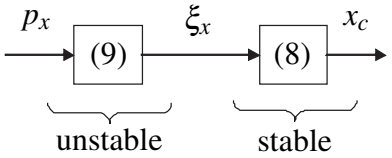

Fig. 4. Coupled dynamics of CP and COM

where $\sigma = [x_c, \dot{x}_c]^T$. The explicit solution of (3) is

$$\sigma(t) = \begin{bmatrix} \cosh(\omega t) & \frac{1}{\omega}\sinh(\omega t) \\ \omega \sinh(\omega t) & \cosh(\omega t) \end{bmatrix} \sigma_o + \begin{bmatrix} 1 - \cosh(\omega t) \\ -\omega \sinh(\omega t) \end{bmatrix} p_x \tag{4}$$

where $\sigma_o = [x_{c,o}, \dot{x}_{c,o}]^T$ is the initial condition of the system.

B. Derivation of the Capture Point

Pratt et al. [8] and Hof [12] independently introduced the Capture Point. This is the point on the floor (Fig. 1), where the robot (modeled as a LIP) has to step to come to a complete rest, which means that the center of mass (COM) is exactly located over the ankle and the horizontal velocity is zero. Pratt et al. derive the CP from the linear inverted pendulum orbital energy. In this paper we provide an alternative derivation of the CP using (4). We search for a point p_x such that the COM position tends towards the position of the ankle p_x when time tends towards infinity. By inserting this information into the first row of (4) we get

$$x_c|_{t\to\infty} = p_x = x_{c,o}\cosh(\omega t) + \frac{\dot{x}_{c,o}}{\omega}\sinh(\omega t) + p_x - p_x\cosh(\omega t) \tag{5}$$

from which we obtain

$$p_x = x_{c,o} + \frac{\dot{x}_{c,o}}{\omega}\ \cancelto{1}{\tanh(\omega t)|_{t\to\infty}} \tag{6}$$

By inserting (6) into the second row of (4) it can be shown that for this choice of p_x the horizontal velocity of the COM tends to zero for $t \to \infty$. The derived point p_x is equivalent to the definition of the Capture Point ξ_x. For a general set of states $\sigma = [x_c, \dot{x}_c]^T$ it is defined as

$$\xi_x = x_c + \frac{\dot{x}_c}{\omega} \tag{7}$$

C. Capture Point dynamics

We derive the system dynamics based on the Capture Point ξ_x and the COM position x_c. Solving (7) for $\dot{x}_c$ we get

$$\dot{x}_c = -\omega\,(x_c - \xi_x) \tag{8}$$

We find that x_c has a stable first-order open loop dynamics with time constant $\frac{1}{\omega}$. By differentiation of (7) and with (8) and (2) we find

$$\dot{\xi}_x = \dot{x}_c + \frac{\ddot{x}_c}{\omega} = \omega\,(\xi_x - p_x) \tag{9}$$

The Capture Point ξ_x has an unstable first-order open loop dynamics. Fig. 4 illustrates the coupling of the two states x_c and ξ_x. By merging (8) and (9) we find an alternative formulation of the systems dynamics

$$\dot{\theta} = \begin{bmatrix} -\omega & \omega \\ 0 & \omega \end{bmatrix} \theta + \begin{bmatrix} 0 \\ -\omega \end{bmatrix} p_x \tag{10}$$

where $\omega = \sqrt{g/z_c}$, $\theta = [x_c, \xi_x]^T$ and p_x is the ZMP.

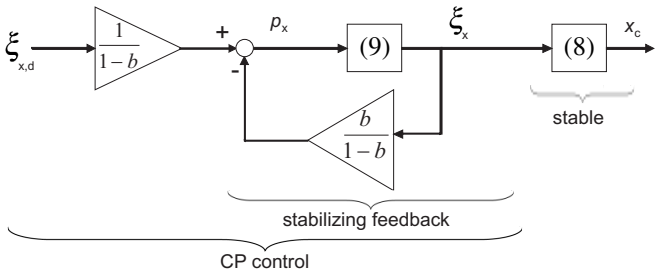

Fig. 5. Stabilization of CP and COM dynamics

III. Capture Point control for bipedal systems

A. Capture Point control using natural dynamics of LIP

In this paper we use a control approach which is motivated by the system structure presented in Fig. 4. As we found that the COM has a stable first-order dynamics (8) and automatically follows the CP, we only consider the CP dynamics (9) to find a control law. The solution of (9) for a constant ZMP p_x is given by

$$\xi_x(t) = e^{\omega t}\,\xi_{x,o} + (1 - e^{\omega t})\,p_x \tag{11}$$

Replacing the initial condition $\xi_{x,o}$ by the current CP ξ_x and reordering (11) leads to the control law

$$p_x = \frac{\xi_{x,d} - e^{\omega\,dT}\xi_x}{1 - e^{\omega\,dT}} = \frac{1}{1-b}\,\xi_{x,d} - \frac{b}{1-b}\,\xi_x \tag{12}$$

where dT is the desired span of time until the arrival of the CP at its desired destination $\xi_{x,d}$ and $b = e^{\omega\,dT}$. The stability of this control law (Fig. 5) will be proven in the following section. The advantage of this control law compared to e.g. pole placement is that in the ideal case (no perturbations and modeling errors) the ZMP stays constant because (11) is equivalent to the natural dynamics of the LIP (with fixed ankle joint). In general it is desirable to hold the ZMP in the middle of the foot. The use of another control law would lead to a non-constant ZMP which increases the danger of tilting (the limit condition being that the ZMP is at the edge of the support polygon). As a real robots dynamics differs from the dynamics of a LIP, the use of (12) leads to a non-constant ZMP, but ensures that the ZMP stays within feasible regions.

B. Two-dimensional CP shifting for bipedal robot control

In a three-dimensional LIP model, both horizontal dimensions x and y have to be taken into account. As their dynamics are independent but equivalent, all equations derived for x in the previous sections can also be applied to the y direction. Therefore, the two-dimensional dynamics of the CP can be derived from (11)

$$\xi(t) = p + e^{\omega t}\,(\xi_o - p) \tag{13}$$

where $\xi = [\xi_x, \xi_y]^T$, $\xi_o = [\xi_{x,o}, \xi_{y,o}]^T$ and $p = [p_x, p_y]^T$. We find that for a constant p the CP moves on a straight line. From (8) we derive the two-dimensional COM dynamics

$$\dot{\mathbf{x}} = -\omega\,(\mathbf{x} - \xi) \tag{14}$$

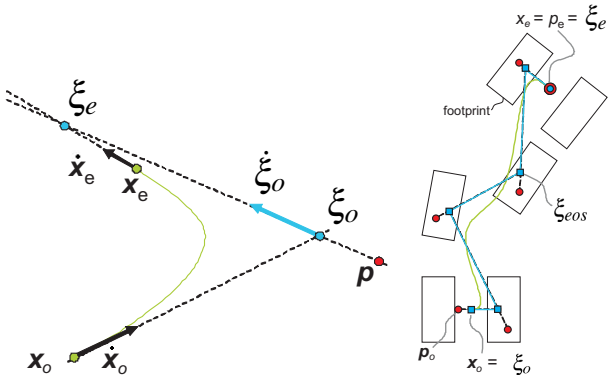

Fig. 6. Two-dimensional Capture Point shifting:
(a) basic shifting mechanism (b) foot to foot shift

From (14) we see that the COM follows the CP, its velocity vector always pointing towards the CP. Fig. 6(a) shows the interrelations between ZMP, CP and COM. For an initial COM state $[\mathbf{x}_o, \dot{\mathbf{x}}_o]$ we find the corresponding Capture Point ξ_o in the direction of $\dot{\mathbf{x}}_o$ (see (7)). The CP ξ is shifted by the ZMP p on a straight line. Its velocity vector points into the same direction as the vector $(\xi_o - p)$. The path of the COM is indicated by the curved line.

The basic idea of the approach we chose is to shift the CP from one footprint of the desired walking path to the next during each step (Fig. 6(b)). The desired CP position at the end of a step is called ξ_{eos}. Its position relative to the ankle was chosen as a constant offset with respect to the ankle. The offset was adjusted such that the resulting ZMP for the ideal LIP dynamics lies within the footprint for all tested walking patterns. An optimized design of the CP offsets will be tackled as a future work. As the COM automatically follows the CP, only the CP has to be considered. In this way, the CP and the COM are shifted from the initial COM position $\mathbf{x}_o$ to the final COM position $\mathbf{x}_e$. ξ_{eos} and the desired time per footstep (t_{step}) are used by the two control algorithms that will be introduced in the next section.

C. CP control approaches

1) CP end-of-step control (CPS): In this approach the desired span of time until CP arrival dT decreases with a slope of $d(dT)/dt = -1$ and is reinitialized ($dT = t_{step}$) at the beginning of each step. Therefore dT has a saw tooth profile (Fig. 7(a)). In contrast to the first control approach, ξ_{eos} is now directly used as the desired Capture Point ξ_d in (12). When the CP is perturbed, the controller tries to apply an appropriate ZMP to shift the CP to the desired final CP position ξ_{eos} within the remaining time dT. In the real application, dT has a lower limit ($dT > dT_{limit} > 0$) because otherwise the gains in (12) would tend towards infinity for very small dT's, which would cause system instability. The control law is not dependent on future step positions or a reference trajectory, but only on the current state of the robot. That makes this approach very attractive for reactive control approaches, such as online step position adjustment

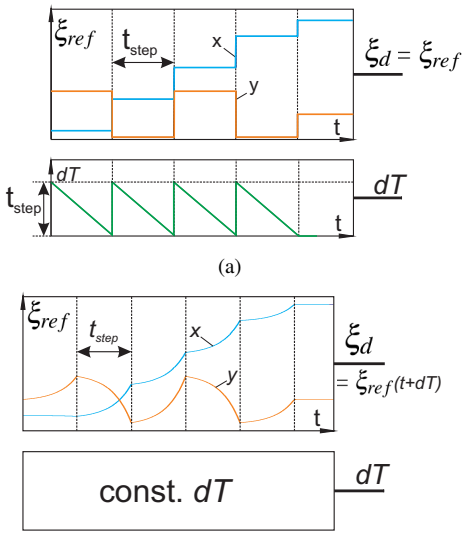

Fig. 7. Generation of desired CP ξ_d and dT patterns:
(a) CP end-of-step control (CPS) (b) CP tracking control (CPT)

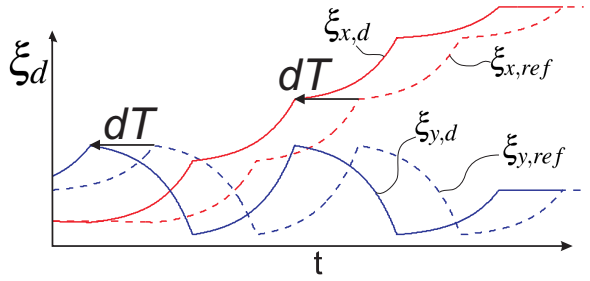

Fig. 8. Forward shifting of CP reference for control with constant dT

(Section VII-.2).

2) CP tracking control (CPT): In this approach, the desired span of time until CP arrival dT is held constant (Fig. 7(b)) whereas the target CP ξ_d follows a reference trajectory ξ_{ref}. ξ_{eos} is used as aiming point for each step (Fig. 6(b)). With ξ_{eos}, the initial CP ξ_o and t_{step} we find the desired ZMP by means of the control law (12). The ideal desired ZMP is a constant point because the LIP model (with constant position of the base joint) is used as reference model. With (13) and the constant desired ZMP we can calculate a reference CP ξ_{ref} for each time step. The basic idea of the control is to shift the CP within a timespan of dT to the position in which the ideal reference CP ξ_{ref} would be at $t+dT$. Therefore, we set $\xi_d(t) = \xi_{ref}(t+dT)$ in (12) (see Fig. 8). In this way, the controller tries to realign the CP with the ideal CP trajectory when the system is perturbed.

D. Tilting avoidance

The desired ZMP p_d produced by the control law (12) is not necessarily located within the support polygon. In order to avoid tilting of the foot, we project p_d to the support polygon. Fig. 9 shows three projection cases. If p_d is within the support polygon (case 1) the projected ZMP p_p is equivalent to p_d. If p_d is outside the support polygon and

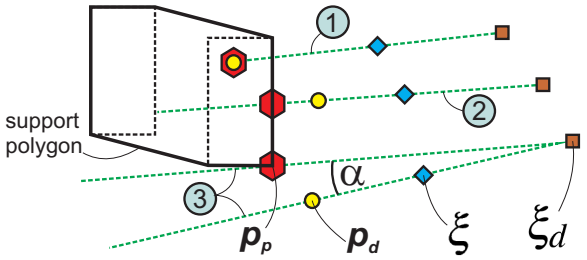

Fig. 9. Projection of desired ZMP to support polygon

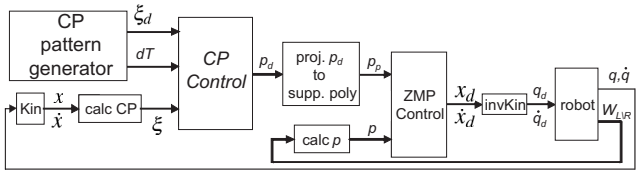

Fig. 10. Capture Point control

the line defined by $(\xi - \xi_d)$ intersects the support polygon (case 2) p_p is chosen as the closest possible intersection point. Otherwise (case 3) p_p is chosen as the point on the support polygon which spans the smallest possible angle α with the desired projection line. In the proposed CP control approach, the only difference between single and double support phase is the changing support polygon, which is handled by the tilting avoidance. Apart from that, there is no difference in the control architecture for both phases. The projection of the desired ZMP p_d onto the support polygon can cause discontinuities in the control signals. Mitigating this problem will be part of future work, although is can not be erased completely, as in the case of a sudden change of the support polygon. The possibility of tilting avoidance by directly limiting the ZMP to the support polygon is an advantage of the CP control compared to other control techniques [2], [5].

E. Overall control loop used for simulations and experiments

Fig. 10 shows an overview of the overall control loop of our bipedal system [10]. The signals $W_{L/R}$ of the 6-DOF force torque sensors (FTS) in the ankles of both legs are used to calculate the ZMP p. By means of a forward kinematics, the position $\mathbf{x}$ and velocity $\dot{\mathbf{x}}$ of the COM are computed from the positions q and velocities $\dot{q}$ of the joints. We insert $\mathbf{x}$ and $\dot{\mathbf{x}}$ into (7) and find the current Capture Point ξ. ξ, ξ_d and dT are used to calculate the desired ZMP p_d (Section III-C). If p_d does not lie within the support polygon it is (to avoid tilting) projected to the support polygon (Section III-D) and called p_p. We currently use a position based ZMP controller to produce the commanded ZMP p_p, but it can be replaced by any other ZMP controller such as a force control based one. The used ZMP controller produces the desired position x_d and velocity $\dot{x}_d$ of the COM, which are translated to the commanded joint angles using the inverse kinematics of the robot.

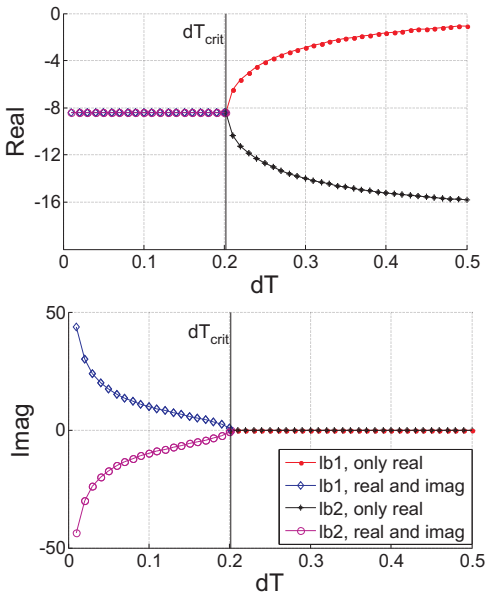

Fig. 11. Real and imaginary parts of eigenvalues $\lambda_{1,2}$ as a function of dT

IV. Stability Analysis

A. Nominal stability

To test the stability of the control law (12) we insert it into (10). This leads to the following closed loop system:

$$\dot{\theta} = \begin{bmatrix} -\omega & \omega \\ 0 & \frac{\omega}{1-b} \end{bmatrix} \theta + \begin{bmatrix} 0 \\ -\frac{\omega}{1-b} \end{bmatrix} \xi_{x,d} \tag{15}$$

where $b = e^{\omega\, dT}$. The eigenvalues of this closed loop are $\lambda_1 = -\omega$ and $\lambda_2 = \frac{\omega}{1-b}$ respectively. λ_1 is always stable and λ_2 is stable for every $dT > 0$. Therefore, the system is globally stable as long as $dT > 0$.

B. Robustness with respect to constant COM error

In a real robot the position of the COM could be inaccurate due to modeling errors, or the exact COM position could be unknown due to loads carried by the robot. To examine the influence of such COM errors on the systems stability and the stationary deviation of the COM, we introduce a measurement error Δx_c:

$$\Delta x_c = x_{c,m} - x_c \tag{16}$$

where x_c is the real and $x_{c,m}$ is the measured position of the COM. As Δx_c is constant, the measured velocity equals the real velocity

$$\dot{x}_{c,m} = \dot{x}_c \tag{17}$$

Using (7) we find the calculated CP $\xi_{x,m}$

$$\xi_{x,m} = x_{c,m} + \frac{\dot{x}_{c,m}}{\omega} = x_c + \Delta x_c + \frac{\dot{x}_c}{\omega} = \xi_x + \Delta x_c \tag{18}$$

Inserting the measured CP into (12) leads to

$$\tilde{p}_x = \frac{1}{1-b}\,\xi_{x,d} - \frac{b}{1-b}\,\xi_{x,m} = \frac{1}{1-b}\,\xi_{x,d} - \frac{b}{1-b}\,\xi_x - \frac{b}{1-b}\,\Delta x_c \tag{19}$$

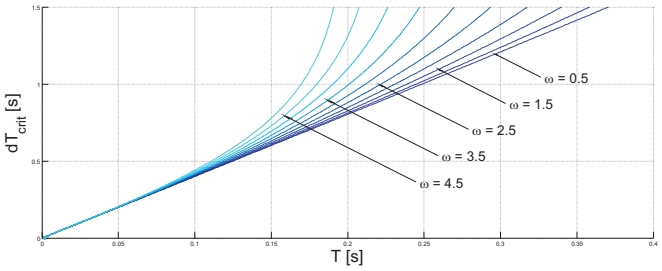

Fig. 12. Dependency of dT_{crit} on T as a function of ω

With (10) and (19) we find the new closed loop dynamics:

$$\dot{\theta} = \begin{bmatrix} -\omega & \omega \\ 0 & \frac{\omega}{1-b} \end{bmatrix} \theta + \begin{bmatrix} 0 \\ -\frac{\omega}{1-b} \end{bmatrix} (\xi_{x,d} - b\,\Delta x_c) \tag{20}$$

The system matrix is not influenced by the COM error (cf. 15) and therefore the system is still globally stable for $dT > 0$.

In steady state the second row of (20) is

$$\dot{\xi}_x = 0 = \frac{\omega}{1-b}\,\xi_x - \frac{\omega}{1-b}\,(\xi_{x,d} - b\,\Delta x_c) \tag{21}$$

Reordering (21) leads to

$$\xi_x = \xi_{x,d} - b\,\Delta x_c = \xi_{x,d} - e^{\omega\, dT}\,\Delta x_c \tag{22}$$

In steady state it holds that $\xi_x = x_c$ (see (8)) and therefore

$$x_c = \xi_{x,d} - e^{\omega\, dT}\,\Delta x_c \tag{23}$$

We find that the steady state solution of the COM position depends on dT.

C. Robustness with respect to ZMP lag

To examine the effect of a lag in the achievable ZMP we introduce a first-order dynamics between the desired ZMP $p_{x,d}$ and the real ZMP p_x as proposed in [3]

$$p_x = \frac{1}{1+sT}\,p_{x,d} \quad or \quad \dot{p}_x = \frac{-1}{T}\,p_x + \frac{1}{T}\,p_{x,d} \tag{24}$$

We define a state vector $\hat{\theta} = [x_c, \xi_x, p_x]^T$ and expand (10)

$$\dot{\hat{\theta}} = \begin{bmatrix} -\omega & \omega & 0 \\ 0 & \omega & -\omega \\ 0 & 0 & -\frac{1}{T} \end{bmatrix} \hat{\theta} + \begin{bmatrix} 0 \\ 0 \\ \frac{1}{T} \end{bmatrix} p_{x,d} \tag{25}$$

Inserting (12) into (25) leads to the closed loop dynamics

$$\dot{\hat{\theta}} = \begin{bmatrix} -\omega & \omega & 0 \\ 0 & \omega & -\omega \\ 0 & -\frac{b}{(1-b)\,T} & -\frac{1}{T} \end{bmatrix} \hat{\theta} + \begin{bmatrix} 0 \\ 0 \\ \frac{1}{(1-b)\,T} \end{bmatrix} \xi_{x,d} \tag{26}$$

The corresponding eigenvalues are

$$\lambda_{1,2} = \frac{\omega T - 1 \pm \sqrt{(1+\omega T)^2 + 4\omega T\,\frac{b}{1-b}}}{2T} = \frac{\omega T - 1 \pm \rho}{2T}$$
$$\lambda_3 = -\omega \tag{27}$$

λ_3 is stable by default whereas $\lambda_{1,2}$ has to be examined in more detail. By means of an analysis of the square root

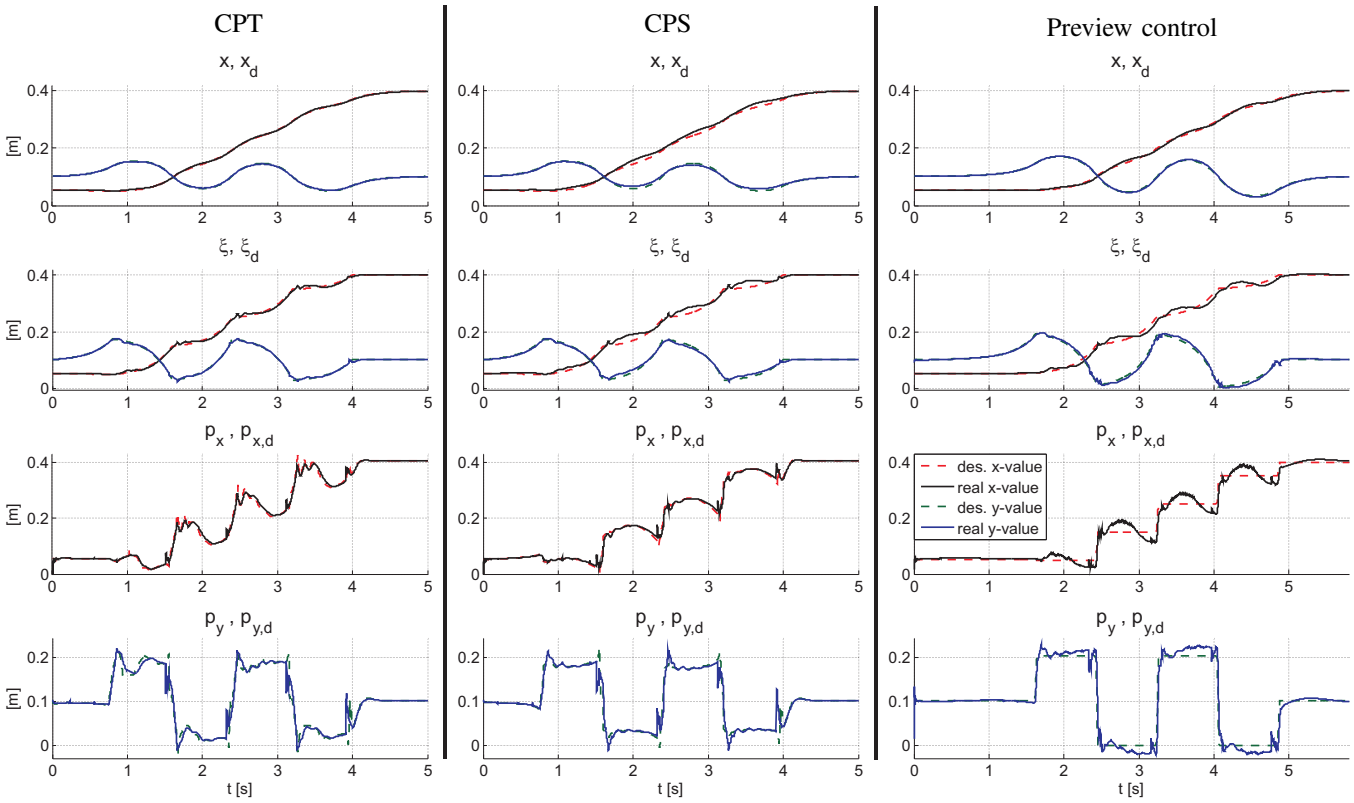

Fig. 13. Simulation results (x, ξ, p) for CP tracking control (CPT, col. 1), CP end-of-step control (CPS, col. 2) and preview control (col. 3)

term ρ we find limits for the periodicity of the solution of (26). The influence of dT on λ is examined by setting $\rho = 0$. We find a critical dT

$$dT_{crit} = \frac{2}{\omega} \ln \frac{1+\omega T}{1-\omega T} \tag{28}$$

For $dT < dT_{crit}$, the real part of $\lambda_{1,2}$ is given by

$$Re(\lambda_{1,2}) \mid_{dT<dT_{crit}} = \frac{1}{2} (\omega - \frac{1}{T}) \tag{29}$$

whereas there exist imaginary parts of $\lambda_{1,2}$. For $dT > dT_{crit}$ it holds that $\rho > 0$ and therefore the eigenvalues have no imaginary parts. For $dT < dT_{crit}$ an overshooting of the Capture Point ξ and the ZMP p relative to ξ_d occurs if a step in ξ_d is applied to (26). For $dT \to \infty$ we find

$$\lambda_1 \mid_{dT\to\infty} = \omega - \frac{1}{T} \tag{30}$$

$$\lambda_2 \mid_{dT\to\infty} = 0 \tag{31}$$

Fig. 11 shows a plot of the eigenvalues $\lambda_{1,2}$ over dT for a particular case where $T = 0.05s$ and $\omega = 3.1421s^{-1}$. Regarding (29) and (30) we find that the system is stable for $T < \frac{1}{\omega}$. The choice of the desired span of time until the arrival dT does not influence the general stability behavior of the system. In other words, the system can not be destabilized by a wrong choice of dT as long as $T < \frac{1}{\omega}$ holds. Fig. 12 shows the dependency of dT_{crit} on T for several ω's. For small T's, dT_{crit} tends towards a straight line with a slope of 4, meaning that dT has to be more than 4 times bigger than T to avoid imaginary parts of the eigenvalues $\lambda_{1,2}$. As a guideline for the design of a CP controller we find that for constant ω and time lag T the desired span of time until the arrival dT should be chosen bigger than but close to dT_{crit} to avoid imaginary parts of $\lambda_{1,2}$.

V. Simulations and Experimental Results

A. Simulations

To verify the performance of the CP controllers, we performed simulations using OpenHRP3 [13]. The proposed controllers are compared to a conventional preview controller [2] as pattern generator, and the underlying ZMP controller is the same as in [5]. As a simple benchmark, all controllers were tested with the same task: the robot should walk forward five steps and then come to a rest. The desired step length was set to 10cm and the desired time per step (t_{step}) to 0.8s. The simulation results are displayed in Fig. 13. In the simulations and the experiments (presented in the next section), dT (Section III-C) was set to $dT_{const} = 50ms$ for the CPT controller (col. 1). In the CPS controller (col. 2), dT was saturated at a lower limit of 50ms, as the control gains would tend towards infinity otherwise. The last column shows the results of the preview controller. In the tested setup, the preview time (future period of time which is taken into account for the control) was set to 1.6s. We find that the preview controllers result in robot action delayed with respect to the CP controllers. The preview control is not based on the CP, the resulting

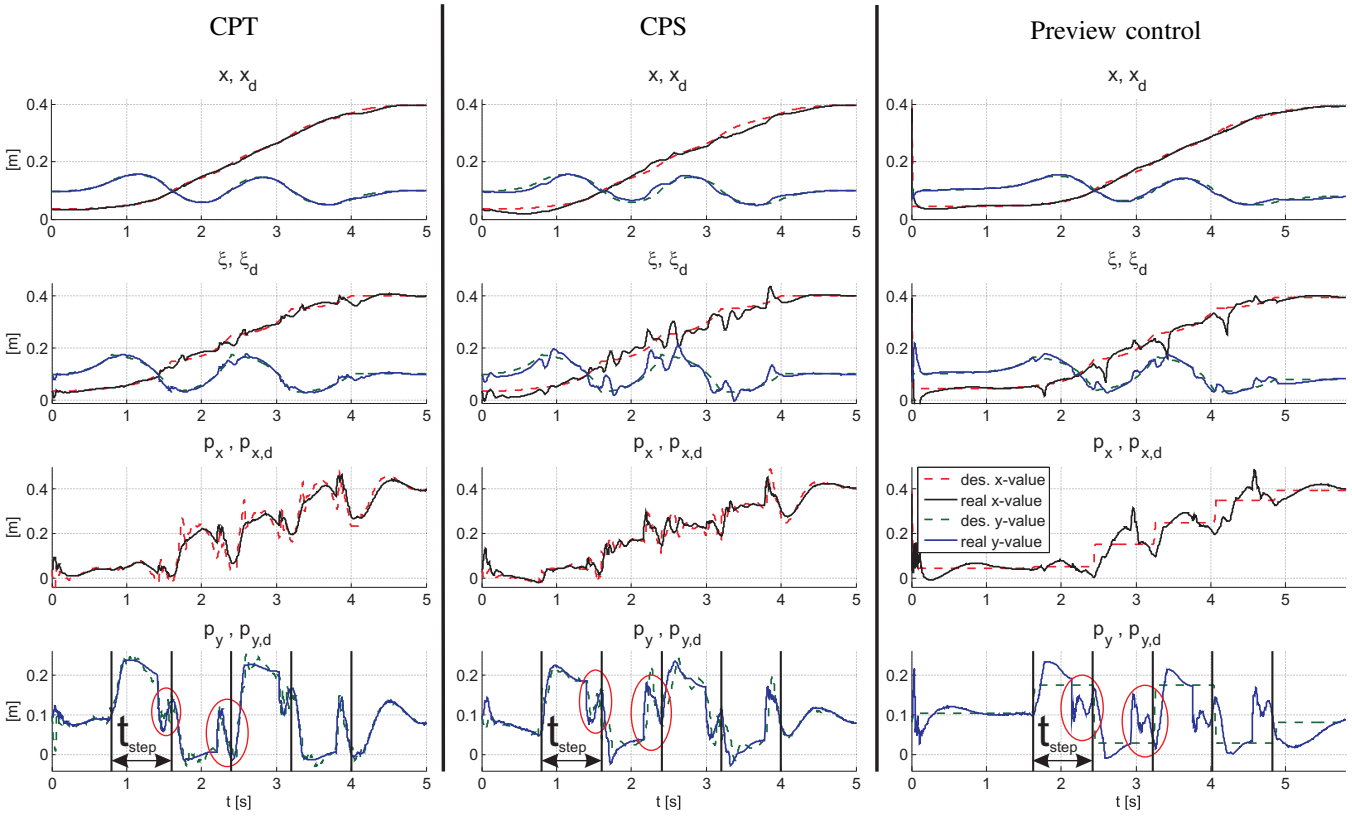

Fig. 14. Experimental results (x, ξ, p) for CP tracking control (CPT, col. 1), CP end-of-step control (CPS, col. 2) and preview control (col. 3)

CP trajectories are only drawn for better comparison of the different controller types. Comparing the ZMP tracking performances of the different controllers, larger ZMP errors for the preview controller compared to the CP controllers can be observed. This is caused by the different control architectures for the two approaches. In the ZMP controller from [5], the ZMP and COM errors are treated as two competing control goals. In contrast to that, the proposed Capture Point controllers have a cascaded structure with outer CP and inner ZMP control loops. We find that the CPT controller (Section III-C.2) shows a very good tracking of the reference trajectories, whereas the preview controller and the CPS controller (Section III-C.1) show larger deviations from the reference COM and CP trajectories. However, the CPS control only uses the desired end-of-step position of the CP (ξ_{eos}, Fig. 6(b)) as its control goal. Temporary perturbations have a smaller effect on the control signal (ZMP) of the CPS compared to the CPT, as the remaining time to compensate for the perturbations is longer for the most part for the CPS. This is the reason for the higher ZMP amplitudes of the CPT. We find that at the end of each step the real CPS trajectories are very close to the reference trajectories. We notice, that the errors of the CP for the CPS control are small in y direction (lateral swinging) whereas the errors in x direction are considerably higher. These higher deviations in x are mainly caused by the influence of the swing legs, which are accelerated mainly in the sagittal plane. It is noticeable, how large the amplitudes of the ZMP in the CPT controller are, especially in x direction. This effect is caused by the higher control gains of the CPT compared to the other control algorithms. Although the CPT can not rely on any previous knowledge of the multi-body effects and has to compensate for them, it shows a good tracking performance.

B. Experiments

The developed control algorithms were tested on the DLR Biped (Fig. 2) [10] in a series of experiments to test their real world performance and the validity of the simulation results. The DLR Biped has six degrees of freedom per leg, a 6-DOF force-torque sensor (FTS) in each foot, position and torque sensors in each joint, and an inertial measurement unit (IMU), which was not used in these experiments. The COM position and velocity is currently estimated by means of the robots kinematics. The task for the robot was exactly the same as in the simulations: walking forward 5 steps with a step length of 10cm and a step time of 0.8s and coming to a rest at the end. The results of the experiments are shown in Fig. 14. The foot trajectories are based on polynomial functions and controlled in open loop (depending on the step length and the stepping time t_{step}). Looking at the y component of the ZMP we find a big influence of the swing leg impact which makes the ZMP move rapidly towards the middle (see encircled details) whereas the desired ZMP is still further outside (best observable for the preview control). The controllers try to compensate for this effect. Especially the CPS with its very low control gains at the beginning of

each step is heavily disturbed by that effect. The preview control is also perturbed considerably (CP plot in Fig. 14 col. 3) whereas the CPT shows the most robust behavior. The premature impact of the swing leg is caused by the tracking errors of the underlying position controller and elastic deflections. The CPT has the lowest errors, although it has the highest ZMP oscillations. We see, that the exploitation of the whole foot area for ZMP control can mean a potential gain in stability and robustness, as long as the tilting condition (ZMP at edge of support polygon) is prevented (Section III-D).

VI. Discussion

The Capture Point (CP) methodology describes the dynamics of a Linear Inverted Pendulum (LIP) in an intuitive way as two cascaded first-order systems. The center of mass (COM) position $\mathbf{x}$ and the Capture Point ξ (Section II-B) are chosen as the system states. By setting the desired end-of-step positions of the CP ξ_{eos} appropriately in the footprints of a desired walking trajectory, the adequate ZMP positions can be found using (12) and desired COM position and velocity (reference) trajectories can be generated with (4), making the CP methodology an alternative to other trajectory generators. By using the ZMP as control signal, a bipedal robot can be stabilized and the CP can be shifted to a desired position.

In this paper, we derived a CP controller (12) based on the natural dynamics of a LIP. One debatable issue is the use of a changing span of time dT until the arrival of the CP at the desired CP end location, as it was used for the controller introduced in Section III-C.1. The changing dT leads to a time-varying system dynamics (15) such that strictly speaking the stability analysis from section IV does not apply. A formal stability analysis for the time-varying case is a future work. The preview matrices of preview controllers [2] are usually computed offline and only valid for one particular height of the COM . In contrast, the CP laws can be applied to any new COM height by only updating the LIP´s time constant ω. Another advantage of the CP based controllers compared to other control strategies [2], [5] is the possibility to limit the commanded ZMP to the current support polygon (Section III-D). This prevents the robot from tilting and allows the use of the whole support polygon as possible commanded position of the ZMP, which means a gain of robustness compared to other approaches. The CPT control (Section III-C.2) proved to be very robust in experiment whereas the CPS control (Section III-C.1) turned out to be more sensitive to perturbations and modeling errors. On the other hand, the CPS is not depending on a reference trajectory but only on the current state, a clear advantage with respect to the CPT which is based on an ideal reference trajectory. Therefore, the CPS is especially attractive for control approaches that require high flexibility of the underlying control and trajectory generation, such as online footprint adjustment and push recovery (Section VII-.2). However, the performance of the CPS needs to be improved. Possible approaches would be the precise identification of the COM model and the use of improved force control for ZMP generation.

VII. Summary and future work

1) Summary: The Capture Point methodology turns out to be an effective and simple tool for the design of trajectory generators and feedback controllers for bipedal walking robots, which was proven by its rigorous use for the control of the DLR Biped [10] in the current work. We could demonstrate the robustness of two CP based control approaches (Sections III-C.2 and III-C.1) in simulations and experiments (Section V).

2) Future Work: Our future work will include (i) extension of CP control for non-constant heights of COM, (ii) online adjustment of footprint positions to increase the robustness of the biped against perturbations, (iii) push recovery, (iv) use of force control for ZMP generation and (v) walking on sloped and uneven grounds.

VIII. Acknowledgments

The authors would like to thank Jerry Pratt and Peter Neuhaus for their initial advice on the Capture Point concept and the fruitful discussions.

References

[1] M. Vukobratovic and J. Stepanenko, "On the stability of anthropomorphic systems," *Mathematical Biosciences*, vol. 15, no. 1-2, pp. 1 – 37, 1972.

[2] S. Kajita, F. Kanehiro, K. Kaneko, K. Fujiwara, K. Harada, K. Yokoi, and H. Hirukawa, "Biped walking pattern generation by using preview control of zero-moment point," in *IEEE Int. Conf. on Robotics and Automation (ICRA)*, 2003, pp. 1620 – 1626.

[3] S. Kajita, M. Morisawa, K. Miura, S. Nakaoka, K. Harada, K. Kaneko, F. Kanehiro, and K. Yokoi, "Biped walking stabilization based on linear inverted pendulum tracking," in *IEEE Int. Conf. on Robotics and Automation (ICRA)*, 2010, pp. 4489 –4496.

[4] T. Sugihara, "Standing stabilizability and stepping maneuver in planar bipedalism based on the best COM-ZMP regulator," in *IEEE Int. Conf. on Robotics and Automation (ICRA)*, 2009, pp. 1966 –1971.

[5] Y. Choi, D. Kim, Y. Oh, and B.-J. You, "Posture/walking control for humanoid robot based on kinematic resolution of CoM jacobian with embedded motion," *IEEE Trans. on Robotics*, vol. 23, no. 6, pp. 1285–1293, 2007.

[6] P.-B. Wieber, "Trajectory free linear model predictive control for stable walking in the presence of strong perturbations," in *IEEE/RAS Int. Conf. on Humanoid Robots*, 2006, pp. 137–142.

[7] S. Kajita, M. Morisawa, K. Miura, S. Nakaoka, K. Harada, K. Kaneko, F. Kanehiro, and K. Yokoi, "Biped walking stabilization based on linear inverted pendulum tracking," in *IEEE/RSJ Int. Conf. on Intelligent Robots and Systems (IROS)*, 2010, pp. 4489–4496.

[8] J. Pratt, J. Carff, S. Drakunov, and A. Goswami, "Capture point: A step toward humanoid push recovery," in *IEEE/RAS Int. Conf. on Humanoid Robots*, 2006, pp. 200–207.

[9] A. L. Hof, "The 'extrapolated center of mass' concept suggests a simple control of balance in walking," *Human Movement Science*, vol. 27, no. 1, 2008.

[10] C. Ott, C. Baumgartner, J. Mayr, M. Fuchs, R. Burger, D. Lee, O. Eiberger, A. Albu-Schaffer, M. Grebenstein, and G. Hirzinger, "Development of a biped robot with torque controlled joints," in *IEEE/RAS Int. Conf. on Humanoid Robots*, 2010, pp. 167 –173.

[11] Y. Sakagami, R. Watanabe, C. Aoyama, S. Matsunaga, N. Higaki, and K. Fujimura, "The intelligent ASIMO: system overview and integration," in *IEEE/RSJ Int. Conf. on Intelligent Robots and Systems (IROS)*, 2002, pp. 2478–2483.

[12] A. L. Hof, M. G. J. Gazendam, and W. E. Sinke, "The condition for dynamic stability," *J. of Biomechanics*, vol. 38, no. 1, pp. 1–8, 2005.

[13] F. Kanehiro, K. Fujiwara, S. Kajita, K. Yokoi, K. Kaneko, H. Hirukawa, Y. Nakamura, and K. Yamane, "Open architecture humanoid robotics platform," in *IEEE Int. Conf. on Robotics and Automation (ICRA)*, 2002, pp. 24–30.